A Semiempirical Quantum Approach to the Formation of Carbon Dioxide Adsorbates on Pt(100) and Pt(111) Cluster Surfaces

C. F. Zinola,[†] C. Gomis-Bas,[‡] G. L. Estiú,[§,||] E. A. Castro,[§] and A. J. Arvia*[,⊥]

Laboratorio de Electroquímica Fundamental, Facultad de Ciencias, Malvín Norte, Montevideo, Uruguay, Departamento de Química-Física, Universidad de La Laguna, Avda. de la Trinidad, 38204 La Laguna, Spain, CEQUINOR, Universidad Nacional de La Plata, Casilla de Correo 962, 1900 La Plata, Argentina, Departamento de Ciencia y Tecnología, Universidad Nacional de Quilmes, Roque Saenz Peña 180, Bernal, Argentina, and INIFTA, Universidad Nacional de La Plata, Sucursal 4, Casilla de Correo 16, 1900 La Plata, Argentina

Received April 20, 1998. In Final Form: April 20, 1998

The geometries and binding energies of CO_2 adsorbates on Pt(100) and Pt(111) cluster surfaces were calculated by means of an improved version of the extended Hückel molecular orbital method. The polarization of the surface by an applied electric potential and coadsorption of H atoms were included in the model. For simulated applied potentials in the range −1.0 to 1.0 V, CO_2 coordination geometries (side-on, formate) involving two adsorbate atoms bonded to the surface are favored, regardless the surface topology and the presence of coadsorbed H atoms. In agreement with experiment, larger binding energies are always calculated for the Pt(100) cluster surface.

1. Introduction

Reactions of CO_2 yielding energy-enriched products, most of them carbon monoxide derivatives such as formaldehyde, formic acid, and carbon monoxide have been studied on several metal electrodes in both aqueous and nonaqueous media.[1−4] The distribution of reaction products depends on the nature of the electrode, the composition of the solution, and other operational conditions.[1,5−7]

The adsorption of CO_2 on metal electrocatalysts[8] is favored when H-adatoms are present on the electrode, as it appears that the formation of CO_2-containing adsorbates, usually denoted as reduced CO_2 adsorbates, requires the simultaneous interaction of CO_2 and H-adatoms. Some of these adsorbates can be detected by anodic stripping voltammetry.

The role of H-adatoms in the formation of reduced CO_2 adsorbates has been studied combining spectroelectrochemical and voltammetric techniques on faceted and polycrystalline Pt and Rh electrodes in aqueous sulfuric acid.[3] For (100)- and (111)-faceted Pt electrodes in acid solutions, two main anodic stripping current peaks have been recorded, which have been related to a weakly and a strongly CO_2 adsorbate. The electrooxidation current peak ratio for these adsorbates depends on the potential sweep rate and solution composition.[9]

The formation of reduced CO_2 adsorbates on Pt from aqueous environments is a surface-structure sensitive reaction, as demonstrated using different types of electrodes.[3,4,9] Thus, in contrast to Pt(111),[10,11] the activity of Pt(100) for this process is relatively high. This crystallographic-face-dependent CO_2 adsorption on Pt can be related to the difference in the electronic characteristics of the electroadsorptive sites and their relative distribution.

The complete anodic stripping of reduced CO_2 adsorbates from Pt has been mainly related to the electrooxidation of CO- and CHO-type adsorbates to CO_2.[1,3,12] Photoelectron spectroscopy has provided interesting results for the formation of both reduced CO_2 adsorbates and their decomposition products, such as formate species on Fe and Ni.[13,14]

Moreover, EMIRS (electrochemical modulated infrared spectroscopy)[15] data have shown the presence of either $H^{\bullet}CO$ or $HCO_2^{\bullet-}$adsorbates, whereas from SNIFTIRS (subtractively normalized interfacial Fourier transform infrared spectroscopy)[12] data, the formation of linear, bridge, and multibonded CO adsorbates on Pt in CO_2-saturated aqueous acid solution has been confirmed. Otherwise, in-situ infrared spectra of CO and CO_2 adsorbates on Pt electrodes are different,[16,17] as the C−O

[†] Laboratorio de Electroquímica Fundamental, Malvín Norte.
[‡] Departamento de Química-Física, Universidad de La Laguna.
[§] CEQUINOR, Universidad Nacional de La Plata.
[||] Departamento de Ciencia y Tecnología, Universidad Nacional de Quilmes.
[⊥] INIFTA, Universidad Nacional de La Plata.

(1) Chandrasekaran, K.; Bockris J. O'M. *Surf. Sci.* **1987**, *185*, 495.
(2) Slater, S.; Wagenknecht, J. H. *J. Am. Chem. Soc.* **1984**, *106*, 5367.
(3) Arévalo, M. C.; Gomis-Bas, C.; Hahn, F.; Beden, B.; Arévalo, A.; Arvia, A. J. *Electrochim. Acta* **1994**, *39*, 793.
(4) Jitaru, M.; Lowy, D. A.; Toma, M.; Toma, B. C.; Oniciu, L. *J. Appl. Electrochem.* **1997**, *27*, 875.
(5) Paik, W.; Anderson, T. N.; Eyring, H. *Electrochim. Acta* **1969**, *14*, 1217.
(6) Kapusta, S.; Hackerman, N. *J. Electrochem. Soc.* **1984**, *131*, 1511.
(7) Liever, C. M.; Lewis N. S. *J. Am. Chem. Soc.* **1985**, *106*, 5083.
(8) Kazarinov, V. E.; Andreev, V. N.; Shelepkov, A. V. *Electrochim. Acta* **1989**, *34*, 905.
(9) Marcos, M. L.; González Velasco, J.; Vara, J. M.; Giordano M. C.; Arvia, A. J. *J. Electrtoanal. Chem.* **1989**, *270*, 205; **1990**, *287*, 99.
(10) Nikolic, B. Z.; Huang, H.; Gervasio, D.; Lin, A.; Fierro, C.; Adzic, R. R.; Yeager, E. B. *J. Electroanal. Chem.* **1990**, *295*, 415.
(11) Hoshi, N.; Mizumura, T.; Hori, Y. *Electrochim. Acta* **1995**, *40*, 883.
(12) Chandrasekaran, K.; Wass, J. C.; Bockris, J. O'M. *J. Electrochem. Soc.* **1990**, *137*, 518.
(13) Wedler, G.; Ganzmann, I.; Borgmann, D. *Appl. Surf. Sci.* **1993**, *68*, 335.
(14) Wambach, J.; Illing, G.; Freund, G. *Chem. Phys. Lett.* **1991**, *184*, 239.
(15) Beden, B.; Bewick, A.; Razaq, M.; Weber, J. *J. Electroanal. Chem.* **1982**, *139*, 203.
(16) Westerhoff, B.; Holze, R. *Ber. Bunsen-Ges. Phys. Chem.* **1993**, *97*, 418.

S0743-7463(98)00447-8 CCC: $15.00
Published on Web 06/05/1998

stretching frequency resulting from CO adsorbates corresponds to a stronger bond than that resulting from reduced CO_2 adsorbates.[18] Furthermore, it has been proposed that CO adsorbates formed from CO_2 electroreduction products may result from the decomposition of a more reactive species such as formate.[19] Therefore, structural conclusions derived from spectroscopic data and mechanistic conclusions derived from electrochemical data for Pt in acids are not fully coincident. This subject becomes, thence, a challenging one that deserves more detailed experimental studies in order to be fully understood.

The calculation of the stability of the most likely adsorbates that can be formed on different Pt surfaces appears as an adequate approach for providing relevant information that helps the understanding of the much more complex situation prevailing at the electrochemical interface. This work is focused, thence, on the possible geometries and binding energies of reduced CO_2 adsorbates on Pt(111) and Pt(100) cluster surfaces at different simulated electric potentials, calculated from a modified version of the extended Hückel molecular orbital method. Because of the complications associated with the experimental system, mainly related to the definition of the electrochemical interface involving reduced CO_2 adsorbates, a simplified model has been chosen. This model considers the initial adsorption of CO_2 on the uncharged Pt surface and the changes of the adsorbate when a simulated electric potential is applied. The relative influences of the negative applied potential and H coadsorption on CO_2 sticking to Pt are then compared. The model allows us to identify the different species that are likely involved in the reduced CO_2 adsorbate formation. The results derived from these calculations are useful, as a first approximation, to discriminate among possible adsorbates and intermediate species involved in either thermal or electrochemical reduction of CO_2 and oxidation of reduced CO_2 adsorbates.

2. Details on the Calculation

2.1. The Calculation Procedure. The extended Hückel molecular orbital (EHMO) method is the simplest calculation procedure that can be used to describe the valence electronic structure, bonding energy, and chemical properties of relatively large transition metal clusters involved in adsorption problems. Despite its simplicity, it is still the choice when dealing with large systems and high atomic numbers. It has been developed by Hoffmann[20,21] to study the structural and electronic properties of systems at a frozen geometry. Improvements of this method, mainly related to the addition of two-body electrostatic terms,[22−27] have made it capable of optimizing the geometry of the adsorbed ensemble within certain limits. In this framework, the energy of the system, E_T, is expressed as

$$E_T = E_{EHMO} + \sum_{\mu} b^o_{\mu}\, VSIP^o_{\mu} + E_R \qquad (1)$$

where E_T stands for the binding energy of the system, calculated as the difference between the noncorrected EHMO total energy (E_{EHMO}) and the addition of the monoelectronic terms that describe the constituents of the system as being infinitely separated and corrected by repulsion. The second term is calculated for the μth atomic orbital, by means of the occupation number (b^o_{μ}) and the valence state ionization potential ($VSIP^o_{\mu}$), which, in absolute value, equals the diagonal terms of the Hamiltonian ($VSIP = -H_{ii}$). The correction implies the addition of the repulsion energy term (E_R) that is evaluated from the contribution of the electrostatic repulsion energies between atoms A and B (E_{AB}),

$$E_R = \sum_{A}\sum_{B<A} E_{AB} \qquad (2)$$

Among the different approaches that have been developed for computing E_{AB},[22−27] we prefer to calculate it as the energy difference between the Coulombic interaction of A and B separated by a distance R_{AB} and the arithmetic mean of A−B and B−A attractive interaction energies.[26,27]

$$E_{AB} = Z_A\, Z_B/R_{AB} - {}^1/_2\, Z_A \int \rho_B(r)/|R_A - r|\, d\, r - {}^1/_2\, Z_B \int \rho_A\,(r)/|R_B - r|\, dr \qquad (3)$$

where Z_i, R_i, and ρ_i are the nuclear charge, position, and electron density of atom i (i = A, B), B being more electronegative than A. Besides, a distance-dependent exponential factor is also included to correct the off-diagonal EHMO matrix elements, which are calculated by the empirical weighted Wolfsberg−Helmholz formula[28] applied to the diagonal Hamiltonian and overlap matrix terms

$$H_{\mu\nu} = {}^1/_2\, K_{AB}\, (H_{\mu\mu} + H_{\nu\nu})\, S_{\mu\nu} \qquad (4)$$

where μ and ν are the μth and the νth orbitals of atoms A and B, respectively.

K_{AB} and δ are adjustable empirical parameters such as $1.4 \le (1 + \kappa) \le 2.5$ and $0.0 \le \delta \le 0.1$ nm. They are related by the equation

$$K_{AB} = 1 + \kappa \exp[-\delta(R_{AB} - r_o)] \qquad (5)$$

K_{AB} is the EHMO K parameter used in the off-diagonal Hamiltonian matrix elements, and r_o is the sum of atomic radii of A and B. Other energy matrix elements are kept as in the conventional EHMO methodology.

2.2. The Model. The preceding calculation procedure was extended to describe the interaction of CO_2 with Pt(111) and Pt(100) cluster surfaces considering the influence of a simulated electric potential and the coadsorption of H-atoms.

High-spin bilayer Pt_N clusters (N= 25, 32), with d bands filled with at least one electron per d orbital, were used to model the Pt(111) and Pt(100) cluster surfaces, respectively (Figure 1). Clusters were geometrically built, keeping constant the Pt−Pt bond length at 0.277 nm, in

(17) Tayuchi, S.; Ohmori, T.; Aramata, A.; Enyo, M. *J. Electroanal. Chem.* **1994**, *369*, 199.
(18) Tayuchi, S.; Aramata, A.; Enyo, M. *J. Electroanal. Chem.* **1994**, *372*, 161.
(19) Czerwinski, A.; Sobkowski, J.; Marassi, R. *Anal. Lett.* **1985**, *18 (A-14)*, 1717.
(20) Hoffmann, R. *J. Phys. Chem.* **1963**, *39*, 1797.
(21) Turner, A. G. *Methods in Molecular Orbital Theory*; Prentice-Hall: Englewood Cliffs, N.J., 1974.
(22) Anderson, A. B. *Surf. Sci.* **1981**, *105*, 159.
(23) Anderson, A. B.; Grantscharova, E. *J. Phys. Chem.* **1995**, *99*, 9143; *J. Phys. Chem.* **1995**, *99*, 9149.
(24) Estiú, G. L.; Maluendes, S. A.; Castro, E. A.; Arvia, A. J. *J. Electroanal. Chem.* **1990**, *284*, 289.
(25) Anders, L. W.; Hansen, R. S.; Bartell, L. S. *J. Chem. Phys.* **1988**, *59*, 5277.
(26) Calzaferri, G.; Forss, L.; Kamber, Y. *J. Phys. Chem.* **1989**, *93*, 5366.
(27) Braendle, M.; Calzaferri, G. *Helv. Chim. Acta* **1993**, *76*, 924.
(28) Wolfsberg, L.; Helmholz, M. *J. Chem. Phys.* **1953**, *20*, 837.

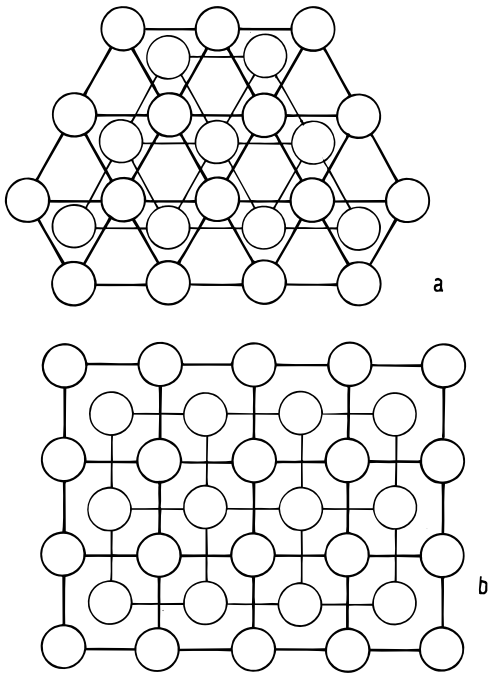

Figure 1. Scheme of the clusters used to model (a) Pt(111) and (b) Pt(100).

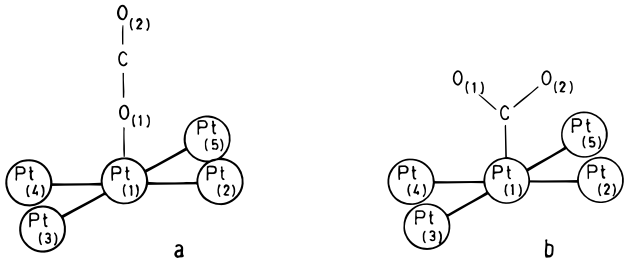

Figure 2. Linear coordination of a CO_2 molecule with a Pt(100) cluster surface (a) bonded through the O atom and (b) bonded through the C atom.

agreement with the interatomic distance of bulk Pt.[29] The multiplicity of the adsorbed ensemble[30] results from interactions with the close shell CO_2 molecule.[31−33]

Coordination of the CO_2 molecule with the Pt surface may involve one or two atoms of the adsorbate and one, two, or more atoms of the substrate. When coordination through a single atom from the adsorbate is considered, the occupation of different Pt adsorption sites defines several adsorption configurations on each Pt cluster, i.e., linear on-top (1-fold), bridge (2-fold), and hollow (higher coordinated sites). Hollow sites are associated with a 5-fold coordination of the adsorbate on Pt(100) (four Pt atoms of the topmost layer and one Pt atom from the underlying layer). For Pt(111), either three or four Pt atoms may define either the (3−1)- or (3−3)-hollow coordination site, depending on the local symmetry of the adsorbate. For each case, the coordination through either the C or the O atom is considered (Figure 2). When two adsorbate atoms are involved in the coordination, two adsorbed species are distinguished, namely, the formate species, which is bound directly through two O atoms

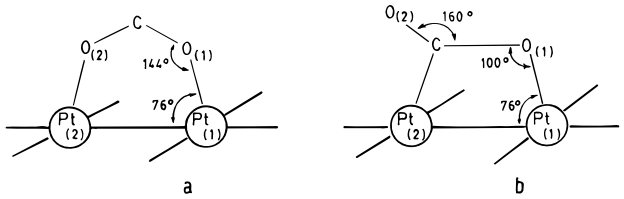

Figure 3. Adsorbate geometries resulting from a two-atom CO_2 coordination on a Pt(100) surface: (a) formate adsorbate; (b) side-on CO_2 adsorbate.

Table 1. EHMO Calculation: Optimized Parameters Based on Pt−O Bond

atomic orbital	VSIP,[a] eV	ζ_1[b]	ζ_2[b]	c_1[c]	c_2[c]
Pt 5d	12.83	4.0950	1.8600	0.7980	0.3520
Pt 6s	9.32	1.9830			
Pt 6p	5.72	1.3440			
C 2s	21.85	2.1600			
C 2p	11.85	2.0750			
O 2s	27.96	2.5640			
O 2p	12.16	2.2640			
H 1s	13.50	1.3000			

[a] VSIP ≡ valence state ionization potential. [b] $\zeta_{1,2}$ ≡ orbital exponents of the base generating functions. [c] $c_{1,2}$ ≡ linear coefficients of the double zeta Pt d-orbitals.

Table 2. EHMO Calculation: Optimized Parameters Based on Pt−C Bond

atomic orbital	VSIP,[a] eV	ζ_1[b]	ζ_2[b]	c_1[c]	c_2[c]
Pt 5d	13.33	4.8950	2.3600	1.2980	0.8520
Pt 6s	9.82	2.4830			
Pt 6p	7.22	2.8440			
C 2s	22.35	2.6600			
C 2p	12.35	2.5750			
O 2s	28.46	3.0640			
O 2p	12.66	2.7640			
H 1s	14.00	1.8000			

[a] VSIP ≡ valence state ionization potential. [b] $\zeta_{1,2}$ ≡ orbital exponents of the base generating functions. [c] $c_{1,2}$ ≡ linear coefficients of the double zeta Pt d-orbitals.

(Figure 3a), and the side-on CO_2 species, which is bound through one C atom and one O atom (Figure 3b).

Equilibrium VSIP values are evaluated in the way previously proposed by Anderson.[23] To consider the polarization of the substrate surface by the CO_2 molecule, the VSIP and Slater exponents are changed until the calculated charges on the atoms for the diatomic bond are close to those predicted by the electronegativity difference resulting from the Pauling's ionicity relationship.[34] This approach has been extensively applied to the study of electrochemical systems.[35−40]

Coordination of CO_2 through either the C or O atom would imply a different polarization of the surface. Different values of VSIP and Slater orbital exponents define, thence, the reference potential of the CO_2−Pt system for coordinations through the C atom (Table 1) and the O atom (Table 2). Values $K_{AB} = 1.75$ and $\delta = 0.035$ render an appropriate description of the equilibrium distances and associated energies with the set of param-

(29) Lide, D. R., Ed. CRC *Handbook of Chemistry and Physics*; CRC Press: Boca Raton, FL., 1990−91.
(30) Zinola, C. F.; Estiú, G. L.; Castro, E. A.; Arvia, A. J. *J. Phys. Chem.* **1994**, *98*, 1766.
(31) Jeung, G. H. *Mol. Phys.* **1988**, *65*, 669.
(32) Jeung, G. H. *Mol. Phys.* **1989**, *67*, 747.
(33) Jeung, G. H. *Chem. Phys. Lett.* **1995**, *232*, 319.
(34) Pauling, L. *The Nature of the Chemical Bond*, 3rd ed.; Cornell University Press: Ithaca, NY, 1992; p 45.
(35) Anderson, A. B.; Awad, M. K. *J. Am. Chem. Soc.* **1985**, *107*, 7854.
(36) Anderson, A. B.; Ray, N. K. *J. Phys. Chem.* **1982**, *86*, 488.
(37) Anderson, A. B. *J. Electroanal. Chem.* **1990**, *280*, 37.
(38) López, M. B.; Estiú, G. L.; Castro, E. A.; Arvia, A. J. *J. Mol. Struct. (THEOCHEM).* **1990**, *210*, 353.
(39) Estiú, G. L.; Maluendes, S. A.; Castro, E. A.; Arvia, A. J. *J. Phys. Chem.* **1986**, *92*, 2512.
(40) Mehandru, S. P.; Anderson, A. B. *J. Phys. Chem.* **1989**, *93*, 2044.

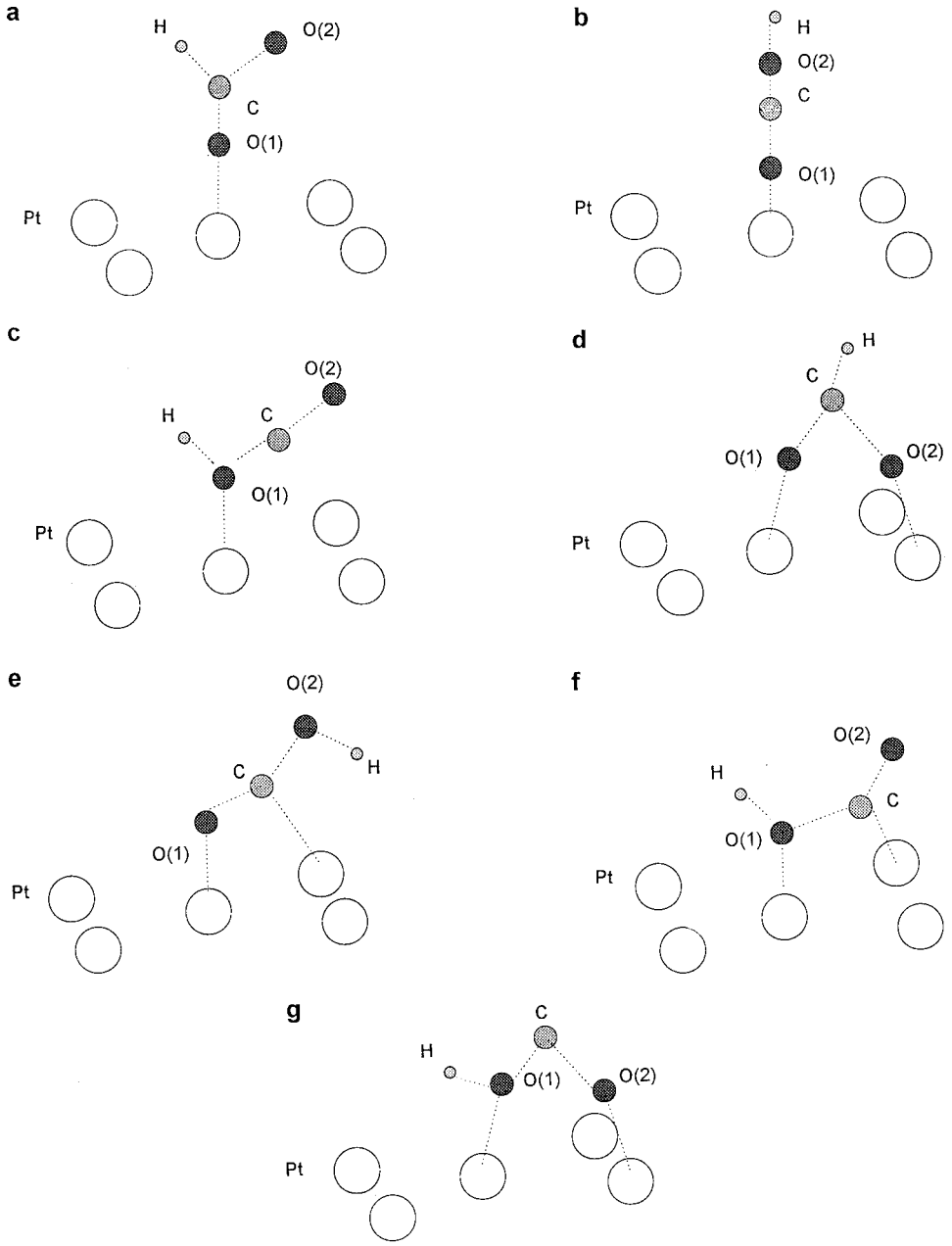

Figure 4. Different CO_2•H adsorbate configurations on a Pt(100) surface: (a) H−C atom coordination; (b) H−O(2) atom coordination; (c) H−O(1) atom coordination; (d) hydrogenated formate adsorbate resulting from bending the O(1)−C-O(2) angle toward a neighbor Pt atom; (e) side on H−O(2)CO adsorbate resulting from bending the O(1)−C-O(2) angle toward a neighbor Pt atom; (f) side on H−O(1)CO adsorbate resulting from bending the O(1)−C-O(2) angle toward a neighbor Pt atom; (g) hydrogenated formate adsorbate with the H atom bound to one O atom.

eters assembled in Tables 1 and 2. When coordination is accomplished through both the C and O atoms simultaneously, the polarization induced by the O atom has been considered in the calculations, as it always renders the most stable structures. For CO_2 and H coadsorption, both species also contribute to modify the electronic density of the Pt surface and, accordingly, the VSIP. Because experimental data on the formation and characteristics of the stable structure of the CO_2−H coadsorbate on Pt are not perfectly known, we have chosen a model that considers the influence of H atoms interacting with adsorbed CO_2 and the surface polarized, thence, by the latter. In this way, the surface polarization induced by the CO_2 molecule and H atom is taken into account by comparing the CO_2 and CO_2•H adsorption without further changes in the physical model.

The applied electric potential is simulated by changing the Fermi energy level of Pt, either decreasing or increasing the absolute value of *VSIP,* from the reference value taken as the potential of zero charge (pzc) of Pt (Table 1), leading to a negative or a positive metal surface charge, respectively.[23] Considering the accuracy of the results obtained in previous investigations,[23,35,36] the correlation between the VSIP shift and the simulated electric potential has been set as 1 (1 V ≡ 1 eV).

The geometry of reduced CO_2 adsorbates has been fully optimized to minimum energy in each case. This implies the simultaneous modification of bond lengths and planar and dihedral angles. Thus, the C−O(1) distance ($r_{O(1)C}$) (Figures 2−4) has been varied stepwise in 0.001 nm until minimum energy was attained. For each fixed value of

Table 3. Binding Energy (BE), Repulsion Energy (ER), Optimized Interatomic Distance (r_{A-B}), and Net Atomic Charge (qA) Values Resulting from Calculations for [Pt(111)•O(1)CO(2)] and [Pt(100)•O(1)CO(2)] at the Reference Potential

	BE, eV	E_R, eV	r_{Pt-O_1}, nm	r_{O_1-C}, nm	r_{C-O_2}, nm	q_{Pt}, eu	q_{Pt}, eu	q_{O_1}, eu	q_C, eu	q_{O_2} eu
					Pt(111)					
on-top	−0.7416	7.30	0.174	0.152	0.110		0.89	0.18	0.02	−0.03
bridge	−0.1679	7.54	0.213	0.127	0.108		1.21	1.02	0.01	0.76
hollow (3−3)	0.0086	10.55	0.154	0.116	0.210			1.52	−0.96	−1.31
hollow (3−1)	0.0559	13.36	0.158	0.120	0.210		−0.30	1.11	−0.92	−1.30
side-on	−3.0184	8.34	0.165	0.228	0.109	0.45[a]	0.72	0.05	−0.13	0.10
formate	−1.4674	8.01	0.194	0.120	0.120		0.98	0.34	−0.23	0.13
					Pt(100)					
on-top	−1.3817	7.50	0.185	0.155	0.110		2.03	0.94	0.25	0.51
bridge	−1.1885	7.34	0.204	0.159	0.105		1.32	0.60	0.04	1.06
hollow	1.0405	7.13	0.185	0.175	0.110		0.41	1.84	−0.86	−1.18
side-on	−3.4305	8.12	0.184	0.191	0.112	0.34[a]	0.82	−0.05	−0.28	0.26
formate	−2.0497	7.90	0.183	0.120	0.120		1.12	0.11	−0.12	0.11

[a] q_{Pt} is the charge of the Pt bound to C atom in side-on coordination.

$r_{O(1)C}$ the remaining internal coordinates were fully optimized.

Adsorption energies (binding energies, BE) were calculated as the difference:

$$BE = E_{T,PtN.X} - E_{T,PtN} - E_{T,X} \quad (6)$$

where $E_{T,PtN}$ and $E_{T,PtN.X}$ stand for the total energy of the [Pt_N] and [Pt_N.X] (X = CO_2, CO_2•H) cluster.

It should be noted that the energy values resulting from semiempirical calculations are not absolute but relative values. They should be considered to analyze trends in the variation of the energy according to modifications produced in the system by changing a variable such as, for instance, the applied electric potential. The parametric condition of the semiempirical procedures led to an overestimation of the binding energy values. It is not only the case of EH calculations, but it is also well-known for neglect of differential overlap (NDO) methodologies, which result in BE values that have to be corrected according to experimental data.[41]

In our case, BE data can be compared to the CO_2−Pt experimental adsorption energy by subtracting 2 eV. The energy scale was normalized considering the BE of CO−Pt calculated by the same procedure, 3.2 eV,[42] and the CO−Pt experimental adsorption energy, which is close to 1.2 eV.[43]

3. Results

3.1. The Interaction of a Single CO_2 Molecule with Pt(111) and Pt(100) Cluster Surfaces. The equilibrium C−O bond length, r_{CO} = 0.118 nm, calculated for free CO_2 is close to the experimental value,[29] that is, 0.120 nm, whereas the calculated dissociation energy is −5.6963 eV, a figure that exceeds published data by 1.6 eV.[29] However, despite this difference, the optimized geometry resulting from the calculation is very accurate. As the semiempirical method is limited for energy value calculations because of their large dependence on the parametrization, attention is focused on the calculated geometries.

3.1.1. CO_2 Adsorption through One Adsorbate Atom. The adsorption of CO_2 on Pt(111) and Pt(100) cluster surfaces involving one atom of CO_2 was studied for the molecule bound to Pt through either the C or O atom, considering for each case the on-top (1-fold), bridge (2-fold), and hollow (multi)-coordination.

In contrast to the adsorption of CO_2 on Pt through the C atom, which always results in a positive value of BE, that is, no stable adsorbate is formed, the adsorption through the O atom leads to stable CO_2 adsorbates.

The geometric characteristics and BE values for stable O-bonded adsorbates are assembled in Table 3. These data show that the linear (on-top) CO_2 adsorption is favored on both Pt(111) and Pt(100) cluster surfaces at the reference potential, as earlier reported by Anderson et al.[44]

For both Pt(100) and Pt(111) cluster surfaces, the on-top adsorption of CO_2 implies the stretching of the O(1)−C bond by 0.03 nm (Figure 2), resulting in a strained C−O(1) single bond.[29] With this stretched bond length fixed, configurations with a tilting of the O(1)−C-O(2) planar angle between 0° and 30° define isoenergetic adsorbates. This result is in agreement with the ab initio calculations about the interaction of CO_2 with a single transition metal atom recently reported by Jeung.[33]

A molecular orbital analysis shows that both the σ and π orbitals of the on-top CO_2 adsorbate are involved in bonding interactions with the d atomic orbitals of adjacent Pt atoms. Then, the CO_2 adsorption bond on both Pt(100) and Pt(111) cluster surfaces can be described as a charge transfer from CO_2 to the Pt cluster, involving a σ-bond reinforced by a π-type Pt(1)−O(1) bond delocalized toward the adjacent O(1)−C bond. However, although an electron transfer from CO_2 to Pt(1) occurs, the Pt atom remains positively charged, as the transferred electron charge is spread throughout the entire Pt cluster. In this case, the O(2) atom is scarcely involved in the adsorption bond, its coordination being mainly related to the extended π-type interaction. Hence, according to the bond distances (Table 3), the O(1)−C bond changes from a double to a single bond because of charge donation. It should be noted that ab initio calculations which describe the CO_2−Pt adsorption interaction defining the metal side by a single Pt atom,[33] also found an ionic character of the bond but a charge transfer from Pt to CO_2. These results are affected to some extent by the absence of Pt interacting atoms, which, without the application of embedding techniques, precludes the spreading of charge over the metal cluster.

The bridge CO_2 adsorbate on both Pt(100) and Pt(111) cluster surfaces involves two Pt atoms interacting with the CO_2 molecule. As the Pt−O bond length is larger

(41) Estiú, G. L.; Zerner, M. C. *Int. J. Quantum Chem.* **1992**, *26*, 587.
(42) Paredes Olivera, P.; Estiú, G. L.; Castro, E. A.; Arvia, A. J. *J. Mol. Struct.* **1990**, *210*, 393.
(43) Campuzano, J. C. In *The Chemical Physics of Solid Surfaces and Heterogeneous Catalysis*; King, D. A., Woodfrusff, D. P., Eds.; Chemisorption Systems, Part A, Elsevier Science Publishers: Amsterdam−New York, 1990; Vol. 3, Chapter 4, p 453.
(44) Ray, N. K.; Anderson, A. B. *Surf. Sci.* **1982**, *119*, 35.

Table 4. Binding Energy (BE) Values at Different Simulated Electric Potentials for Adsorbates Resulting from One Atom CO_2 Coordination on Pt(111) and Pt(100)

Pt(100)

potential	on-top	bridge	hollow	side-on	formate
1.0	−0.5156	−0.3639	1.8964	−6.9113	−5.1158
0.8	−0.6649	−0.4543	1.7052	−6.0131	−4.6831
0.6	−0.8543	−0.6769	1.5131	−5.6457	−3.9757
0.4	1.0904	−0.8849	1.3868	−4.8322	−3.4321
0.2	−1.2015	−1.0021	1.2043	−4.0132	−2.0497
0	−1.3817	−1.1885	1.0405	−3.4305	−2.0497
−0.2	−2.1519	−1.9490	0.5016	−3.8681	−2.1649
−0.4	−2.8986	−2.7050	0.2143	−4.1516	−2.2751
−0.6	−3.2526	−3.2119	−0.0191	−4.4452	−2.3627
−0.8	−3.8020	−3.8476	−0.4543	−4.8983	−2.4331
−1.0	−4.1600	−4.3519	−0.8980	−5.0844	−2.5662

Pt(111)

potential	on-top	bridge	hollow-(3−1)	hollow-(3−3)	side-on	formate
1.0	−0.3046	−0.1459	1.5634	1.3452	−5.6775	−4.5757
0.8	−0.3678	−0.1467	1.3467	1.0347	−5.0131	−4.0341
0.6	−0.4247	−0.1478	1.1378	0.8734	-4.8751	−3.7757
0.4	−0.5467	−0.1519	0.8543	0.5523	−4.1254	−2.9872
0.2	−0.6154	−0.1537	0.2043	0.2189	−3.6732	−2.2561
0	−0.7416	−0.1679	0.0559	0.0086	−3.0184	−1.4674
−0.2	−1.4534	−0.9278	−0.2466	−0.2239	−3.7681	−1.6336
−0.4	−2.0478	−1.6781	−0.4557	−0.3345	−4.1021	−1.8248
−0.6	−2.7681	−2.3467	−0.5931	−0.5432	−4.3458	−1.9072
−0.8	−3.8341	−3.9341	−0.7183	−0.7345	−4.4917	−2.0982
−1.0	−4.5224	−4.3519	−0.8980	−1.0945	−4.6263	−2.1212

than that in the 1-fold coordination, a less effective charge transfer from CO_2 to the Pt cluster occurs, resulting in a less stable adsorbate (Table 3).

The adsorptive CO_2−Pt interaction at both (3−3)- and (3−1)-hollow sites implies a substantial contribution of repulsive interactions, and accordingly, the calculated values of BE correspond to unstable adsorbates (Table 3).

Let us consider the influence of the Pt cluster polarization by an external potential on the value of BE. Data assembled in Table 4 show that, regardless the geometry and topology of the surface, the adsorption is favored by negatively charging. The effect becomes more relevant for the bridge coordination, which reverses the stability relative to on-top for values close to −1.0 V on Pt(100).

The (3−3)- and (3−1)-hollow CO_2 adsorbates remain unstable for simulated electric potentials higher than −0.8 V for Pt(100) and −0.4 V for Pt(111) (Table 4). These adsorbates are less stable than the on-top and bridge adsorbates even at −1.0 V on both Pt cluster surfaces. The fact that the adsorption of CO_2 on Pt is favored when Pt clusters are negatively charged agrees with the experimental data derived from the necessity of covering the H-adatom potential region for the CO_2 adsorption.[8,9,11,12]

Both the Pt−O(1) and O(1)−C bond lengths decrease as the applied potential is negatively shifted, because the charge transfer becomes less effective. These changes in bond length have a negligible influence on the C−O(2) bond over the −1.0 to 1.0 V simulated electric potential range. For bridge CO_2 adsorbates, the value of the O(1)−Pt-Pt angle changes from 66° to 58° for Pt(100), and from 68° to 57° for Pt(111) when the simulated electric potential goes from 1.0 to −1.0 V. Simultaneously, the value of the Pt−O(1)−C angle varies from 114° to 122° on Pt(100) and from 112° to 123° on Pt(111), by changing the simulated electric potential within the same range. The optimized geometric parameters of CO_2 adsorbates on both Pt cluster surfaces at different applied potentials are available upon request.

3.1.2. CO_2 Coordination through Two Adsorbate Atoms. When the adsorption of CO_2 on Pt involves two adsorbate atoms, two species can be formed, namely, a formate adsorbed species that is bound directly through two O atoms (Figure 3a) and a side-on CO_2 species that is bound through the C and one O atom (Figure 3b). Formate adsorbates have been experimentally detected on metal surfaces by means of spectroscopic techniques,[1] whereas the existence of side-on adsorbates has been concluded from infrared emission spectroscopy during hydrocarbon oxidations on Pt.[45]

Binding energy data for formate and side-on CO_2 adsorbates on the Pt(100) and Pt(111) cluster surfaces are assembled in Table 3. For both adsorbates, the BE values depend on the applied potential, defining minimun stabilization at 0 V. However, regardless of the simulated potential, side-on CO_2 adsorbates become the most stable ones on both Pt cluster surfaces. Data assembled in Table 4 show that the stabilization of the side-on CO_2 adsorbate on Pt(100) is always substantially higher than that on Pt(111), and the corresponding BE differences decrease as the applied potential is negatively shifted.

As previously mentioned, the greatest stability of the adsorbates at 1.0 V is due to a charge transfer from CO_2 to Pt, which results in a charge on the molecule that is around +0.36 for the Pt(111) surface and +0.6 for the Pt(100) surface. The reverse charge-transfer process is responsible of the stabilization at −1.0 V. This is reflected in a negative charge for the adsorption of CO_2 on Pt which is again larger for Pt(100) (−0.53) than for Pt111) (−0.17). These figures justify, also, the larger stabilization on the Pt(100) surfaces.

3.2. The Interaction of a Single CO_2 Molecule with the Pt(111) and Pt(100) Cluster Surface in the Presence of H Atoms. The influence of a H atom of the environment on the stabilization of CO_2 adsorbates has been extensively discussed in relation to the mechanism of CO_2 electrooxidation on Pt.[1−5,9−14] Therefore, the calculation procedure previously described was extended to determine the geometry and BE values of the most likely adsorbates that might result from the coadsorption of CO_2 and H on Pt(100) and Pt(111) cluster surfaces. In this way, the occupation of on-top, bridge, and hollow sites by H and on-top, bridge, hollow, side-on, and formate sites by CO_2 have been considered simultaneously, to compare the binding energies of the different resulting CO_2•H adsorbates as well as their evolution under the influence of an applied electric potential. In all the cases, full geometry optimizations were performed in order to find out the characteristics of the most stable adsorbed structures. The results from these calculations are assembled, for the uncharged surfaces, in Table 5.

Coadsorption of hydrogen with formate species define the most stable structures on both Pt surfaces, followed by the system associated with the on-top coordination of both adsorbates. For these, most stable structures, the coordination of H with a Pt atom adjacent to CO_2 has been compared with the direct coordination to either the C or O atoms of the adsorbed CO_2 molecule (Figure 4). For both the formate and the on-top linear CO_2 coordinations, the direct bonding of H to the C atom of the adsorbed molecule stabilizes the system relative to the adjacent adsorption of both species. In the case of formate, the system is stabilized in 1.0 eV on Pt(100) and 0.6 eV on Pt(111) by hydrogen migration to the C atom of the CO_2 molecule, whereas for the case of linear coordination the

(45) Uetsuka, H.; Watanabe, K.; Iwade, T.; Kunimori, K. *J. Chem. Soc., Faraday Trans.* **1995**, *91*, 1801.

Table 5. Values of BE for CO_2 and H Adsorbates on Pt(111) and Pt(100) at the Reference Potential

Pt(100)			Pt(111)		
H-atom	CO_2	BE/eV	H-atom	CO_2	BE/eV
on-top	on-top	−3.0129	on-top	on-top	−2.4560
on-top	bridge	−2.8567	on-top	bridge	−2.2324
on-top	hollow	−1.9786	on-top	hollow(3−3)	−1.0954
on-top	formate	−3.5589	on-top	hollow(3−1)	−1.0002
on-top	side-on	−2.6651	on-top	formate	−3.4254
			on-top	side-on	−2.4123
bridge	on-top	−2.9929	bridge	on-top	−2.3456
bridge	bridge	−2.7547	bridge	bridge	−2.1325
bridge	hollow	−1.6723	bridge	hollow(3−3)	−0.9456
bridge	formate	−3.4531	bridge	hollow(3−1)	−0.8751
bridge	side-on	−2.3197	bridge	formate	−3.3278
			bridge	side-on	−2.1966
hollow	on-top	−1.7531	hollow(3−1)	on-top	−1.5623
hollow	bridge	−1.5673	hollow(3−1)	bridge	−1.1211
hollow	hollow	−0.3489	hollow(3−1)	hollow(3−3)	−0.3632
hollow	formate	−2.0146	hollow(3−1)	hollow(3−1)	−0.1435
hollow	side-on	−1.8831	hollow(3−1)	formate	−1.9433
			hollow(3−1)	side-on	−1.7675
			hollow(3−3)	on-top	−1.2378
			hollow(3−3)	bridge	−0.9864
			hollow(3−3)	hollow(3−3)	0.0123
			hollow(3−3)	hollow(3−1)	0.0924
			hollow(3−3)	formate	0.1029
			hollow(3−3)	side-on	0.4099

Table 6. Values of BE for CO2.H Adsorbates on Pt(111) and Pt(100) Surfaces at the Reference Potential

Pt(100)			Pt(111)		
H-atom	CO_2	BE/eV	H-atom	CO_2	BE/eV
on-top	on-top	−3.0129	on-top	on-top	−2.4560
H−CO_2 (f)		−4.5782	H−CO_2 (f)		−4.1233
H−O(2)CO (t)		−2.8431	H−O(2)CO (t)		−2.2143
H−O(1)CO (t)		−2.9973	H−O(1)CO (t)		−2.2241
on-top	formate	−3.5589	on-top	formate	−3.4254
H−OCO (f)		−3.1192	H−OCO (f)		−3.0637
H−CO_2 (t)		−3.5435	H−CO_2 (t)		−3.2138

[a] where H−CO_2 (f) refers to H bound to C atom of formate species, H−OCO (f) refers to H bound to one O atom of formate species, H−CO_2 (t) refers to H bound to C atom of on-top species (Figure 4a), H−O(2)CO (t) refers to H bound to the O(2) atom of on-top species (Figure 4b), H−O(1)CO (t) refers to H bound to one O(1) atom of on-top species (Figure 4c).

system is stabilized in 1.5 and 1.7 eV respectively, for the uncharged surface, as concluded from data shown in Table 6. Moreover, for the latter, a formate adsorbate is formed by bending the Pt(1)−O(1)−C angle (Figure 4d). At the reference potential, this process requires an activation energy that is AE = 0.04 eV for Pt(100) and AE = 0.08 eV for Pt(111). These values of AE become zero when the simulated electric potential is lower than −0.4 eV for both Pt surfaces.

Coordination of the H atom to the O atoms of the adsorbed CO_2 molecule leads to less stable structures than those defined by direct H−Pt interaction (Figure 4b,d). Furthermore, the bending of either the Pt(1)−O(1)−C or O(1)−C−O(2) angles in the H−O(2)CO adsorbate would result in a hydrogenated side-on CO_2 adsorbate (Figure 4e). The values of AE for this change in the adsorbate configuration are AE = 0.20 eV for Pt(100) and AE = 0.22 eV for Pt(111). These values of AE decrease to zero (−0.2 V downward) when the simulated electric potential is shifted negatively. Similarly, the bending of the Pt(1)−O(1)-C and O(1)−C-O(2) angle of the H−O(1)CO adsorbate would generate a new hydrogenated side-on CO_2 adsorbate (Figure 4f). The values of AE for this process are AE = 0.14 eV for Pt(100) and AE = 0.17 eV for Pt(111). These values of AE decrease to zero (−0.3 V downward) as the simulated electric potential is negatively shifted.

Values of BE and their dependence on the simulated electric potential for the different adsorbates can be seen in Table 7. The stability of these adsorbates decreases from −1.0 to 0 V and then increases again from 0 to 1.0 V, although the greatest stability is observed at −1.0 V. The explanation for the potential dependence of BE values was already discussed in section 3.1.2.

Summarizing, when H atoms are considered in the definition of the electrochemical interface, the coordination of a H atom with the CO_2 adsorbate leads to the formation of formate adsorbates, on both Pt(100) and Pt(111) cluster surfaces over the potential range covering from the reference potential downward. Hydrogen coordination may imply the direct attachment to the C atom of an adsorbed formate species or the bending of a linearly bonded C-hydrogenated CO_2 one. This fact suggests that formate species are the most likely adsorbed intermediates formed in the electrochemical reaction of CO_2 on Pt.

4. Conclusions

According to our calculations, CO_2 adsorption on Pt(100) and Pt(111) surfaces implies the simultaneous coordination of two atoms of the molecule, to give side-on and formate configurations. This result might be valid in the experimental potential range including the pzc (potential of zero charge) and the H-adatom potential region. Among these configurations, and regardless the simulated potential, side-on CO_2 adsorbates become the most stable ones on both Pt surfaces. In agreement with experiment, larger BE are always calculated for the Pt(100) cluster surface.

When H-atoms are also considered in the definition of the electrochemical interface, formate adsorbates become the most stable ones. Because it appears that the formation of CO_2-containing adsorbates requires the simultaneous interacion of CO_2 and H adatoms, our

Table 7. Values of BE for Adsorbates Resulting from CO_2 and H on Pt(111) and Pt(100) Surfaces at Different Simulated Electric Potentials (V)

	Pt(100)			Pt(111)		
pot.	H on-top CO_2 formate	H on-top CO_2 on-top	H−CO_2(f)	H on-top CO_2 formate	H on-top CO_2 on-top	H−CO_2(f)
1.0	−4.8563	−5.4432	−6.7576	−4.6679	−4.7543	−6.4332
0.8	−4.6751	−4.8466	−6.2323	−4.4540	−4.4430	−6.0443
0.6	−4.3242	−4.4320	−5.9768	−4.2544	−3.9311	−5.7548
0.4	−4.0875	−3.9654	−5.1288	−3.9912	−3.2352	−4.9867
0.2	−3.7456	−3.6543	−4.9769	−3.6743	−2.7658	−4.7564
0	−3.5589	−3.0120	−4.5782	−3.4254	−2.4560	−4.1233
−0.2	−3.9654	−3.5431	−5.0123	−3.7876	−2.7435	−4.7475
−0.4	−4.3547	−4.1333	−5.8675	−4.0923	−3.2431	−5.2912
−0.6	−4.8244	−4.7654	−6.5457	−4.6765	−3.9652	−5.7348
−0.8	−5.3765	−5.4350	−7.0913	−5.0230	−4.4432	−6.3754
−1.0	−5.7452	−5.7545	−8.4243	−5.4439	−5.0618	−7.1309

calculations suggest that hydrogenated formate species are the most likely adsorbates formed in the electroformation of reduced CO_2 on Pt.

Acknowledgment. This work was financially supported by the Consejo Nacional de Investigaciones Científicas y Técnicas (CONICET), and Comisión de Investigaciones Científicas de la Provincia de Buenos Aires (CIC), Argentina. C.F.Z. is a member of the Research Career at Programa de Desarrollo de Ciencias Básicas (PEDECIBA), Uruguay. G.L.E. gratefully acknowledges the University of Quilmes for a research grant.

LA980447+